2013

Wind loading on trees integrated with a building envelope

Aly Mousaad Aly
aly@lsu.edu

et al .

Recommended Citation

Aly, A.M. et al. "Wind loading on trees integrated with a building envelope," Wind and Structures, 17(1), 69-85, 2013. DOI:10.12989/WAS.2013.17.1.069

Wind loading on trees integrated with a building envelope

Aly Mousaad ALY[*, a,b,c,d], Alberto Zasso[a], Girma Bitsuamlak[c,d], Alberto Franchi[a], Pietro Crespi[a], Nicola Longarini[a] and Arindam Gan Chowdhury[d]

[a]*Politecnico di Milano, Milano, Italy*
[b]*Alexandria University, Alexandria, Egypt*
[c]*Western University, Ontario, Canada*
[d]*Florida International University, Florida, USA*

Abstract. With the sustainability movement, vegetated building envelopes are gaining more popularity. This requires special wind effect investigations, both from sustainability and resiliency perspectives. The current paper focuses on wind load estimation on small- and full-scale trees used as part of green roofs and balconies. Small-scale wind load assessment was carried out using wind tunnel testing in a global-effect study to understand the interference effects from surrounding structures. Full-scale trees were investigated at a large open-jet facility in a local-effect study to investigate the wind-tree interaction. The effect of Reynolds number combined with shape change on the overall loads measured at the base of the trees (near the roots) has been investigated by testing at different model scales and wind speeds. In addition, high-speed tests were conducted to examine the security of the trees in soil and to assess the effectiveness of a proposed structural mitigation system. Results of current research show that small-scale testing may overestimate wind loading on actual trees when the tests do not account fully for tree-wind interaction. On the other hand, the full-scale testing shows that at higher wind speeds the load coefficients tend to be reduced, limiting the wind loads on trees. No resonance or vortex shedding was visually observed.

Keywords: green building envelope; full-scale testing; tall buildings; tree; wind loading; wind tunnel

1. Introduction

An important contemporary architectural goal is to consider the health of people in city centers where, for instance, green spaces moderate the impact of human activities by absorbing pollutants and releasing oxygen (Hough 1984). In addition, green envelopes help to maintain a certain degree of humidity in the atmosphere, improve the urban climate by acting as coolers and regulators (moderate temperature), contribute to the maintenance of a healthy urban environment

[*] Corresponding author, [a] Visiting Researcher, [b] Assistant Professor, [c] Research Fellow, [d] Former Research Associate, Ph.D., Email: aly.mousaad@polimi.it; aalysaye@uwo.ca

Note: This is the preprint of the manuscript and should be cited as follows.

Aly, A.M. et al. "Wind loading on trees integrated with a building envelope," Wind and Structures, 17(1), 69-85, 2013. DOI:10.12989/WAS.2013.17.1.069

by providing clean air, and also preserve the balance of a city's natural urban environment (Baycan-Levent and Nijkamp, 2009). With the sustainability movement, vegetated building envelopes are gaining more popularity. It is becoming common to see buildings with green envelopes. High-rise buildings are also being built to satisfy sustainability criteria, at the same time maintaining other architectural requirements. Not only small plants and flowers can be planted into buildings' envelope, but large trees could also be introduced for tall buildings' roofs and balconies. This new direction of sustainability requires an in-depth understanding of the processes behind the occurrence of wind-induced damage to trees, which might become an additional source of wind-borne debris. This understanding is of interest to structural engineers, architects and forest ecologists. Decisions related to risk management also require information about the wind loading on trees and the wind-tree interaction.

There have been significant efforts by researchers to understand the behavior of trees under wind loading (Diener et al., 2009; Haritos and James, 2008; Hu et al.,2008a, 2008b, 2011; Kontogianni et al., 2011; Lin et al., 2009; Zubizarreta-Gerendiain et al., 2012). James (2003) carried out field measurements of dynamic forces on trees, branches, and cables in an attempt to quantify the magnitude of the wind-induced forces and to provide a basis for evaluating tree stability. The results show that the dynamic response of the tree involves a complex interaction of the natural frequencies of each component of the tree, including the trunk, main branches, sub-branches, and smaller sections. James et al. (2006) described a dynamic model of a tree, incorporating the dynamic structural properties of the trunk and branches. The results they reported indicate that sway is not a harmonic, but is very complex due to the dynamic interaction of branches. The branch mass contributes to dynamic damping which acts to reduce the detrimental harmonic sway motion of the trunk and so minimizes loads and increases the mechanical stability of the tree. Spatz et al. (2007) recorded damped oscillations of a Douglas fir (Pseudotsuga menziesii) tree and its stem without branches. They noticed that all large branches had nearly the same frequency as the tree. This property is responsible for the distribution of mechanical energy between stem and branches and leads to an enhanced damping. Gilman et al. (2008) investigated the effects of different pruning techniques on trunk movement on live oaks subjected to hurricane force winds. They compared tree movement in wind on non-pruned trees with movement on trees with crowns thinned, reduced or raised. They concluded that foliage and branches toward the top of tree crowns were largely responsible for trunk movement in straight-line wind. Trees with crowns thinned or reduced would have less damage in windstorms. Sellier and Fourcaud (2009) investigated the sensitivity of tree aerodynamic behavior to the material and geometrical factors characterizing the aerial system. They used a finite element analysis to simulate the mechanical response of a 35-year-old maritime pine (*Pinus pinaster*, Pinaceae) subjected to static and dynamic wind loads. The results of the finite element simulations show that tree deflections and responses to high winds are more sensitive to changes in the geometry of tree axes, including length, diameter, and insertion angles, than to alterations of material properties (different types and shapes of trees were used).

The purpose of the current study is to assess the wind loads exerted on model and real prototype trees tested for a typical vegetated building envelope. Wind loads on model-scale trees were measured in a boundary-layer wind tunnel in a global configuration considering the architectural features of the hosting buildings as well as other surrounding structures. Wind loads on larger trees (3-4 m high) were measured individually under full-scale wind speeds at a Wall of Wind testing facility, Florida International University (Aly et al., 2011). This multi-scale study was proposed to better understand the overall wind loads exerted at the root of trees both for

model and actual trees. While the small-scale study permits understanding the interference effects from surrounding structures (global study), the larger tree study allows the investigating of the wind-tree interaction and shape change (with wind speed change) effects on the force coefficient. Experimental high-speed tests were also conducted on real trees to test a proposed wind-damage mitigation mechanism.

2. Methodology

2.1 Model-scale wind tunnel testing (global test)

Small-scale trees mounted on two vegetated buildings named tower D and tower E were tested at the Politecnico di Milano wind tunnel in an effort to estimate the overall wind loads exerted on the trees (Fig. 1). Fig. 2 shows the mean wind speed and turbulence intensity profiles used in the wind tunnel study. The wind-induced total force coefficient was estimated on small-scale (1:100) trees mounted on tall buildings. Note that the term 'total force coefficient' is used in the current paper rather than the term 'drag coefficient'. This is because of the uncertainty of the wind speed directionality, on a tree located on a building, which is affected by the surrounding structures. The 'total force' is the resultant of the 'drag force' and the 'lift force'. In fluid dynamics, drag refers to forces which act on a solid object in the direction of the relative fluid flow velocity (French, 1970). Lift is the component of force that is perpendicular to the oncoming flow direction. The projected areas of four arbitrary trees were estimated as shown in

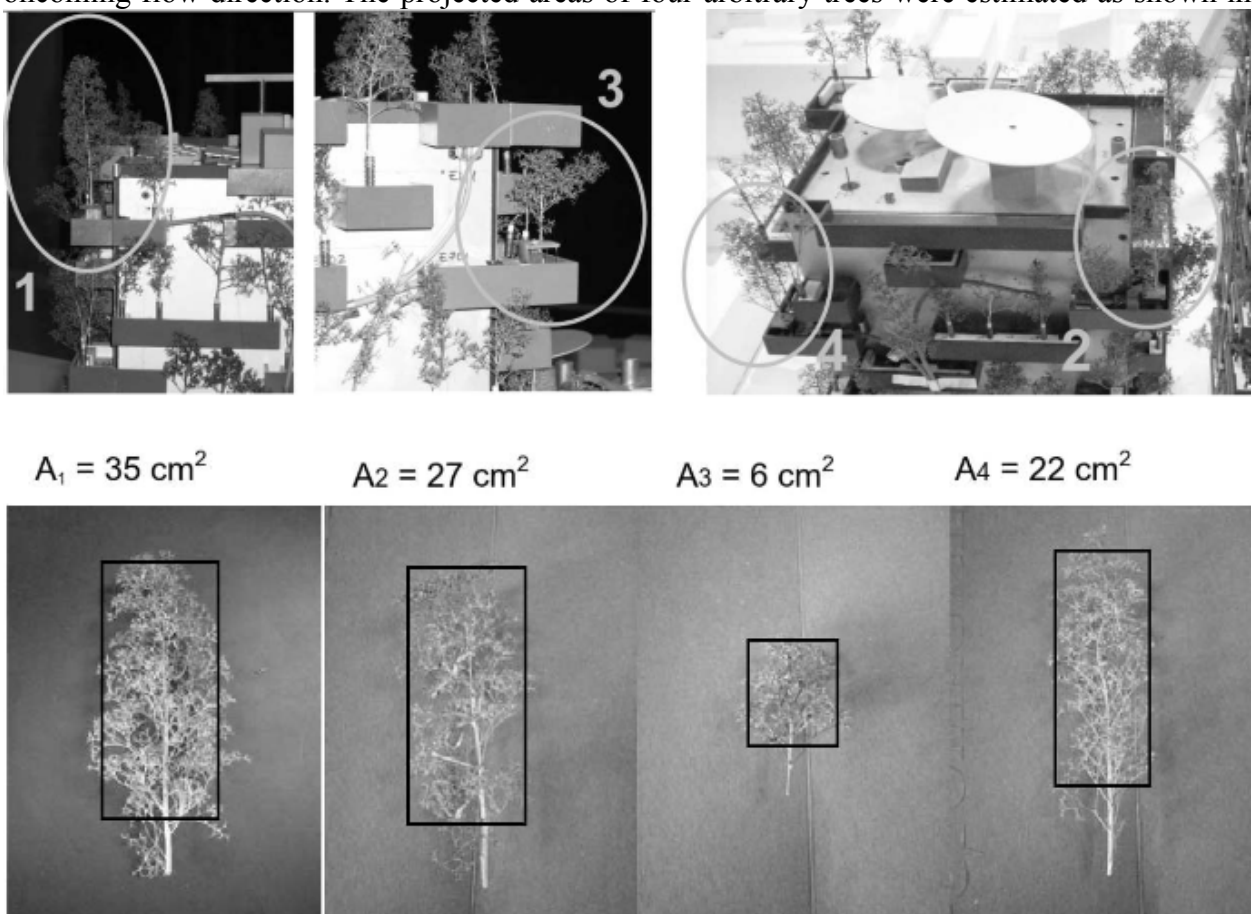

Fig. 3. The two towers tested have been modeled in 1:100 scale with their surroundings. The towers D and E were manufactured as a 'rigid aerodynamic model' that is a static model reproducing the geometry of the full-scale structure (aerodynamic surfaces and its details). The model of the building includes the trees on the terraces. Wind forces are measured by purpose-built dynamometers (Fig. 1-b). The instrument measures the components of the force parallel to the plane of the floor. Measurements of wind force coefficients were carried out on four trees placed in four different locations on the model (on balconies at different places and very close to the roof). All tests were run for a wind tunnel velocity (U = 6.3 m/s) at a reference height of 1 m. The Reynolds number at small-scale can be calculated as follows:

$$\mathrm{Re} = \frac{\rho_a \times U \times D}{\mu_a} \tag{1}$$

where ρ_a = air density (1.2 kg/m^3); U = mean wind velocity (m/s); μ_a = air dynamic viscosity (1.85 x 10^{-5} Pa.s); D = characteristic dimension (0.035 m). The above equation gives Re = 1.43 x 10^4.

2.2 Full-scale Wall of Wind testing (Phase 1)

In order to account for Reynolds number and shape change effects, full-scale trees (i.e. real trees) were tested at Florida International University's Wall of Wind (WoW). The 12-fan WoW was chosen for the present study for at least three reasons: (1) the facility could achieve the target design wind speed (38 m/s), (2) the wind field measures 6 m wide × 4.5 m high (at the exit of the WoW), which was large enough to accommodate large-sized trees of interest and (3) the open-jet flow was ideal for testing trees that may potentially shed their leaves or fail under the applied wind without posing the risk of damaging the fans in a closed circuit facility such as used for the small-scale testing. The WoW facility allows for simulating wind speeds in excess of 50 m/s. Fig. 4 shows the mean wind speed profile and turbulence intensity profile used in this study. Although different wind profiles were developed using a small-scale replica of the WoW facility (Aly *et al.,* 2011a, 2011b, 2012), the wind profile used in this study was uniform based on the assumption that such uniformity is representative of the wind profile over a floor height portion of full-scale tall building where a tree is located. Simulating the whole atmospheric boundary-layer (ABL) profile for this specific component study was deemed not to be a critical requirement.

Four trees of different species were chosen for the full-scale study. Tree # 1: Gumbo Limbo (*Bursera simaruba*); Tree # 2: Bay Rum (*Pimenta recemosa*); Tree # 3: Green Buttonwood (*Conocarpus erectus*); Tree # 4: Pigeon Plum (*Coccoloba diversifolia*). Pictures of the trees are

shown in

(a) (b) (c) (d)

Fig. 5. Table 1 lists the measured dimensions for each tree tested. A steel frame was used for holding the tree (without roots) on load cells in an effort to estimate the overall wind load acting on the full-scale trees. The fabricated steel frame mounted on the load cells is shown in Fig. 6. Wind-induced reactions were measured at the base of the trees using four multi-axis load cells (45E15A4 250 lb) provided by JR3, Inc. (http://www.jr3.com/). Each load cell is capable of measuring (simultaneously) six components of loadings (three forces and three moments) along and about three orthogonal axes. The nominal accuracy for all axes is 0.25 %. A sampling rate of 100 Hz was used. For each tree tested in Phase 1, the trunk of the tree was first cut near the roots and then inserted into the steel frame. Once inserted in the steel frame, each tree was visually rotated so that the largest branch area would be arranged perpendicular to the oncoming wind, yielding the highest expected wind loading on the tree.

A mitigation system that consists of steel cable was proposed for the trees as a technique to enhance the security of the tree during extreme wind. One steel cable was mounted vertically beside the test set (vertical strand); another cable was attached between the vertical cable and the tree at its mid-height (see Fig. 7-b). Two tests were conducted: in the first test the cable between the tree and the vertical cable was attached, and in the second test the cable was removed [here after referred as without the mitigation cable 'w/o' and with the mitigation cable (w)]. Base line measurements were taken before and after each individual test to eliminate the effect of initial loads, measured by the strain gauges, which ascertained the accuracy of the measurements. Different test wind speeds were considered for testing: 12.8 m/s (low wind speed), 26.2 m/s (medium wind speed) and 40 m/s (design wind speed). In addition, 46 m/s, 49.5 m/s and 53 m/s were used for high-speed testing. All the measured forces were collected at a sampling rate of 100 Hz for a duration of 180 s for each of the three lowest wind speeds and for a duration of 10 s for the high-speed tests.

2.3 Full-scale testing at higher wind speed (Phase 2)

The designer of the building proposed different mitigation techniques to maintain security of the trees under strong wind. These techniques include: (1) steel cage designed to transmit the loads from the roots of the tree to the concrete planter to avoid any possible overturning of the

tree (see

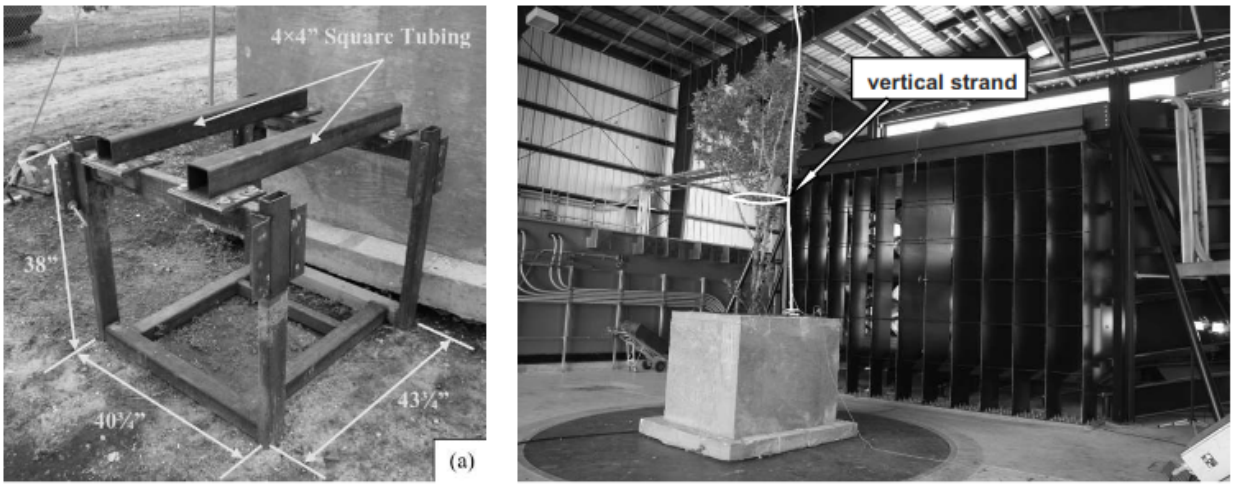

(a) **(b)**

Fig. 7-a); (2) vertical steel cable to prevent the tree from falling over the balcony's terrace, in case of failure (see

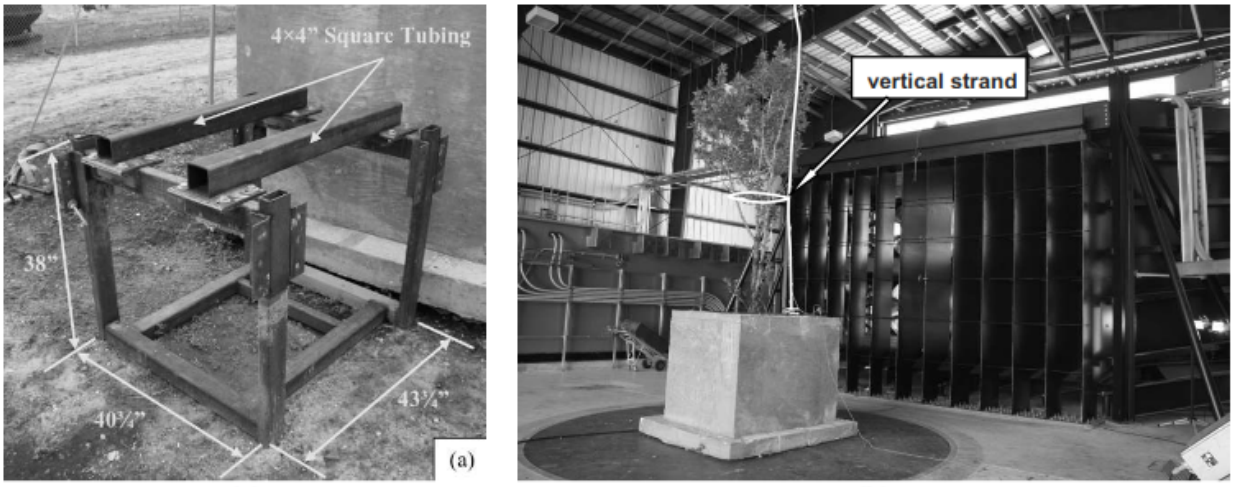

(a) **(b)**

Fig. 7-b). To determine the viability of the concrete planter box and the steel cage for securing the tree under the applied wind loads, and to investigate the effectiveness of the vertical safety strand concept for mitigating the tree deflection, high-speed testing was carried out (Phase 2). Another purpose of this testing was to check whether such a mitigation technique would be

indeed necessary.

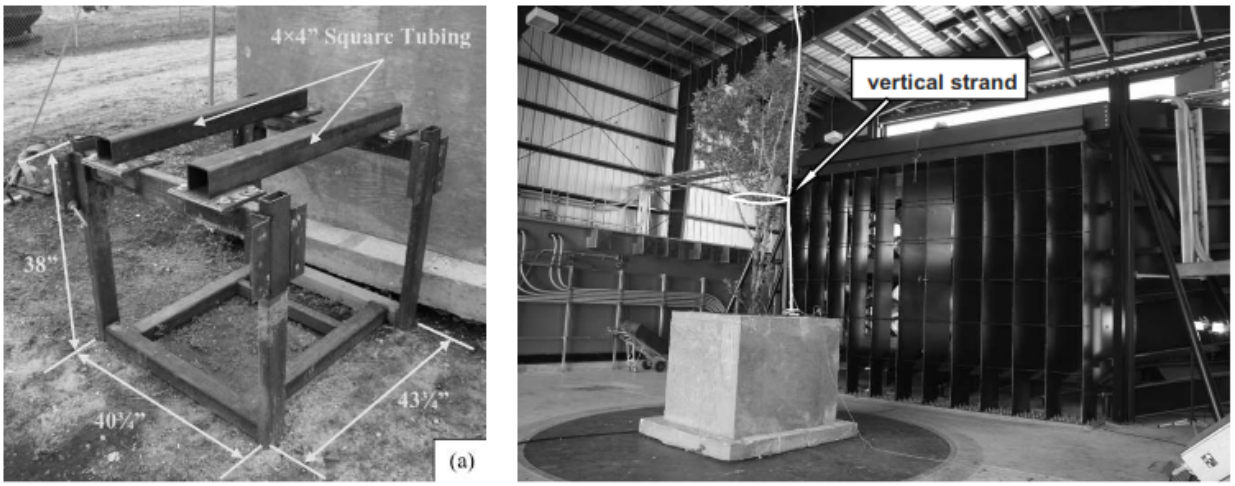

(a) **(b)**

Fig. 7 shows a sectional model of the balcony where a typical tree can be mounted. This section was fabricated using reinforced concrete with similar full-scale dimensions. The high-speed tests were carried out in the following scenarios:

(1) Tree in a concrete box with steel frame and mitigation cables: in this case, different wind speeds were considered: 12.8 m/s (low wind speed), 26.2 m/s (medium wind speed) and 40 m/s (design wind speed), in addition to 46 m/s, 49.5 m/s and 53 m/s for high-speed testing. For each of the first three wind speeds a duration of 180 s was allowed. Since a smooth wind flow was used in this study (as Phase 1), a longer time duration was not necessary. Wind loads in the mitigation cable were measured during the test.

(2) Tree in a concrete box with steel frame and without mitigation cable: Similar tests described in step (1) were carried out except the mitigation cable was removed, and hence no force measurements were available.

(3) Tree in a concrete box without steel frame and without mitigation cables: Similar tests designated in step (2) were carried out without the steel frame. The tree was just placed in the soil inside the planter box.

The overall load components evaluated at the base of the tree for both small- and large-scale testing are presented in non-dimensional coefficients as follows:

$$C_{TOT} = \frac{F_{TOT}}{0.5\, r_a U^2 A} \tag{2}$$

where ρ_a = air density (1.2 kg/m^3); U = reference mean wind velocity (m/s); A is the projected area of the tree. The reference wind speed U for wind tunnel tests (global study) was measured at 1 m height in the upstream wind, immediately at the entrance of the turntable. This height corresponds to 100 at full-scale. For WoW tests (local study), the average wind speed at tree's mid-height was considered. Similarly, the overturning moment coefficient C_M in along-wind direction can be expressed as:

$$C_M = \frac{F_{TOT}}{0.5\, r_a U^2 A H} \tag{3}$$

where H is tree's height.

3. Results

Fig. 8 shows the mean total force coefficient versus the wind direction angle for small-scale trees tested in the boundary-layer test section (Re = 1.43 x 10^4). Tree # 1 is subjected to higher wind loads than trees # 2, 3, and 4. This is because tree # 1 is located close to the roof with fewer interference effects from the building (see

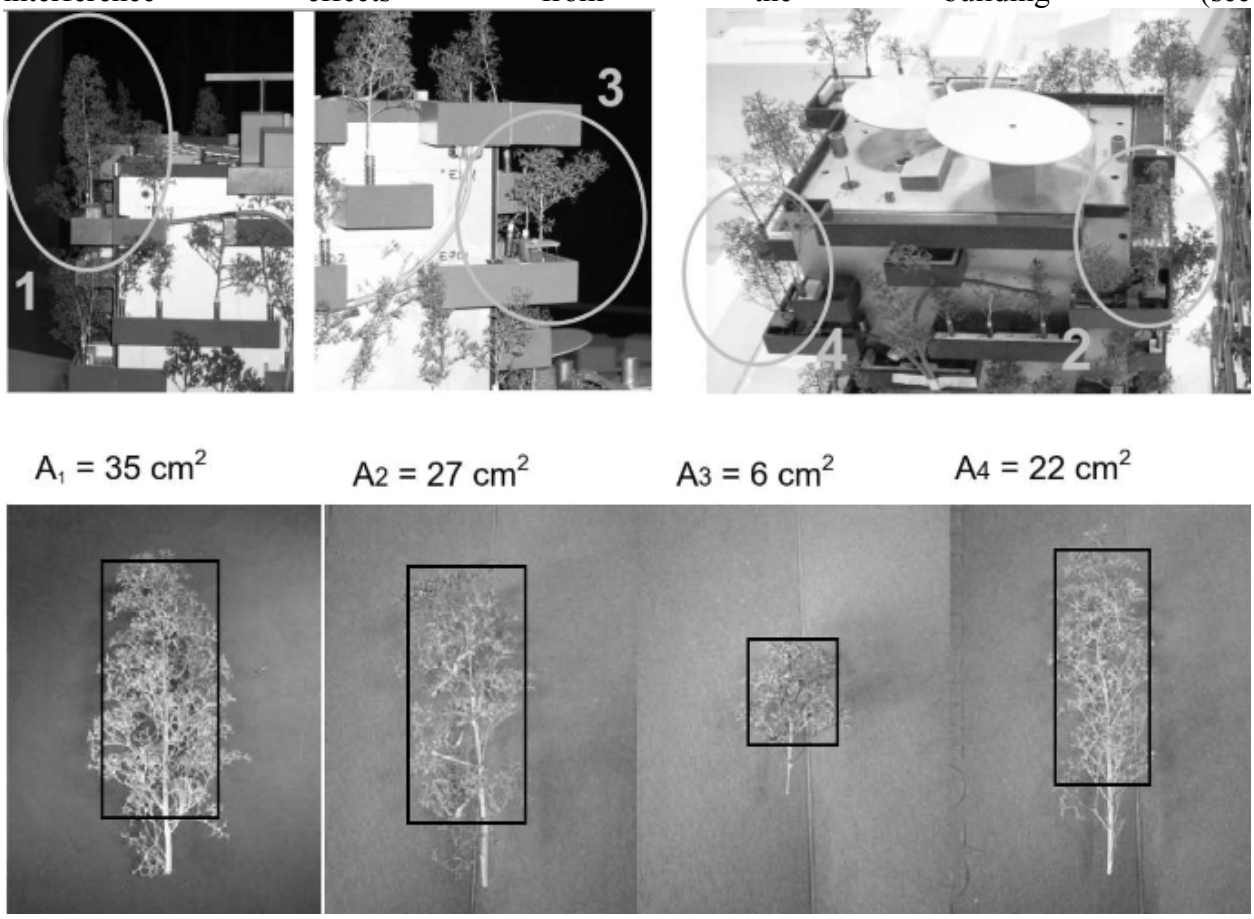

Fig. 3). The other three trees, however, are subjected to lower wind loads as a result of the sheltering effects by the building itself as well as the surrounding buildings. The mean value of the total force coefficients in small-scale wind tunnel testing can be as high as 0.8. Fig. 9 shows the root mean square of the total force coefficient versus wind direction angle. Tree # 1, which is mostly uncovered by surrounding structures, is subjected to the highest root mean square loads.

Large-scale test results are shown in Figures 10-15. Fig. 10 shows the mean values of the total force coefficient versus wind speed (Phase 1). The corresponding Reynolds numbers vary from 1.18 x 10^6 to 4.89 x 10^6. This means that the Reynolds number at full-scale is about two orders of magnitude larger than that at the small-scale. It is to be recalled that two types of testing were carried out in Phase 1: trees mounted on a steel frame without the vertical mitigation cable 'w/o' and trees mounted on the steel frame and attached to the mitigation cable (w). Generally, when the safety cable was attached to the tree, it resulted in a reduction of the total force coefficient. However, there is a significant reduction in the mean force coefficient with increase in the wind speed. This is predominantly attributed to the associated shape change as the tree tends to bend more at higher wind speeds in a way that limits the increase in the loads with

the wind speed (see Fig. 11). Such a phenomenon was not correctly modeled at small-scale as the artificial trees used in the wind tunnel tests were not suitable for a realistic aero-elastic type of response. It is also interesting to notice that at very low wind speed, the force coefficient is close to the value predicted by wind tunnel tests on the tree #1 (subjected mostly to the wind loads with less effects from the surrounding structures, see

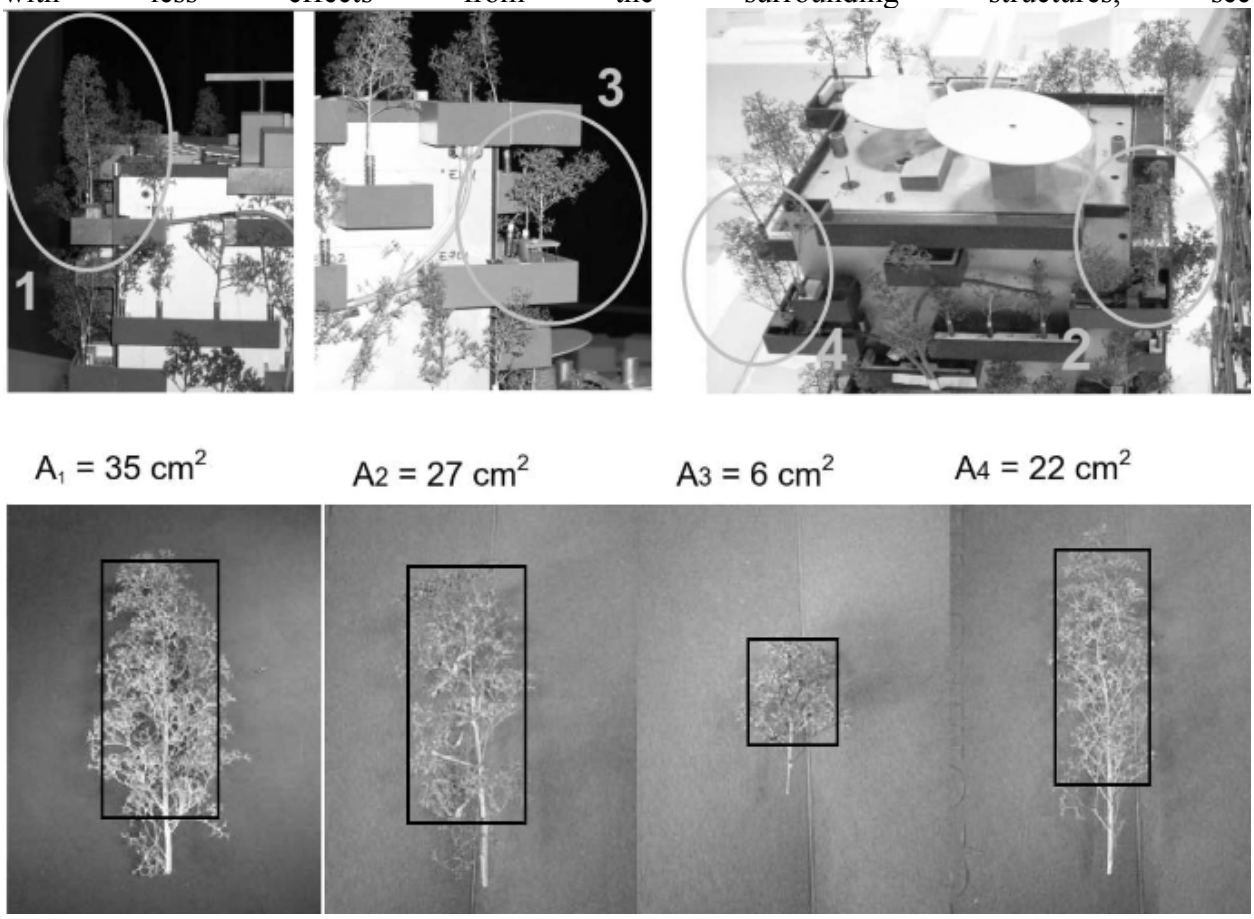

Fig. 3). Fig. 12 shows root mean square total force coefficient versus wind speed for large-scale trees tested at the WoW (Re varies from 1.18×10^6 to 4.89×10^6). It is shown that the root mean square values of the force coefficient are very low with respect to the values obtained from the wind tunnel tests. This is dominantly because for this testing the wind turbulence was not simulated and smooth flow conditions were used at the WoW.

The trend of the moment coefficient C_M with the wind speed is very similar to the trend of the force coefficient C_{TOT} (see Fig. 13). Again, when the safety cable was attached to the tree, it resulted in a reduction of the moment coefficient. Nevertheless, there is a significant reduction in the mean values of the moment coefficient with increase in the wind speed. This is predominantly attributed to the associated shape change as the tree tends to bend more at higher wind speeds in a way that limits the increase in the loads with the wind speed. Such shape change resulted into reduction in the projected area as well as shifting of the moment arm.

Fig. 14 shows the tension force created in the vertical safety cable versus wind speed for actual trees tested at the WoW (Phase 1). It is worth to mention that the cross-wind loads measured by the load cells were very low; by testing over a range of wind speeds, no resonance or a coherent vortex shedding was visually observed. The tree leaves/branches dampened all kinds of potential instability.

Table 3 lists the values of the load exerted in the vertical safety strand for the tree # 3 mounted in the concrete planter box (Phase 2). Fig. 15 shows minor cracks noticed after the high-speed tests carried out in Phase 2. This represents the worst observed soil cracking during Phase 2 testing. This was the test case with 90° wind direction without the safety strand and without the top 4×4" steel members installed on the steel frame inside the planter box.

4. Discussion

4.1 Comments on the results

At small-scale, since the trees were made of different materials other than the full-scale one, it was hard to change the wind speed and go to higher wind speeds as the process was accompanied by shape change. So both shape change and Reynolds number effects are combined together and it was not possible to separate one effect from the other. That is why a very low wind speed (6.3 m/s) was taken at the wind tunnel. However, at full-scale, different wind speeds were considered. The results indicate the importance of shape change (see Fig. 11). It was difficult to distinguish Reynolds number effects from shape change effects (with wind speed change) as they are coupled together.

The wind tunnel study was a global study, in which the interference effect of surrounding structures were considered, since that effect was dependent on the wind direction angle, there was no unique local wind speed to be used as a reference. Practically, the designer of the building refers to the mean wind speed at a reference height for design purposes. On the other hand, the WoW testing was a local study, where such interference effects were not taken into account. The main purpose of the WoW tests was to verify possible shape changes leading to reduced wind loads.

The torsion mode of failure is basically dependent on the shape of the tree. It can be important for asymmetric and large trees, however, for the trees considered in the current study, these effects were minimum. Mostly the tree responded in bending as indicated in Fig. 11. Perhaps some significant torsional modes will be noticed in future tests in a turbulent flow. The designer of the building proposed different mitigation techniques to maintain security of the trees under strong wind (steel cage and vertical safety strands). The results of the high-speed tests carried out in Phase 2 at the WoW shows that the mitigation mechanism, steel frame and vertical cable, is not a requirement for this design. It is worth mentioning that the role of the steel rope is to prevent the tree falling down, out of the terrace in case of failure. It is not supposed to have any function in controlling the displacements of the tree. The low values of the tensile force in the strand are in accordance to the design. On the other hand, the steel cage was supposed to avoid a possible overturning of the tree, but such failure has been demonstrated to be very unlikely by the experimentation.

An important non-dimensional parameter commonly used in mechanics of fluid-structure interactions is the Cauchy number (Blevins, 1990). According to de Langre (2008), the Cauchy number C_Y can expressed as

$$C_Y = \frac{r_a U^2}{E} S^3; \qquad S = \frac{H}{d} \tag{4}$$

in which ρ_a is the air density, U is the mean wind speed, E is the modulus of elasticity, S is the slenderness ratio defined as the ratio of the maximum to minimum cross-sectional dimensions of

the system H and d. For ρ_a of 1.25 kg/m^3, S = 3.45/.065= 53 (tree # 4) and E of 10^8 Pa, corresponding to soft living vegetal tissues, de Langre (2008), the Cauchy number can be ranging from 0.3 to 5.23 under the range of wind speed tested (12.8 m/s to 53 m/s). This means that the Cauchy number can be larger than 1, therefore, one can expect a significant static deformation of the trees under the action of wind (de Langre, 2008). A useful parameter for understanding the dynamics of structures under wind is the reduced velocity, U_R, which is defined as the ratio of the period of free vibration of the solid, T, over the advection time, d/U. The reduced velocity is expressed as

$$U_R^2 = C_Y S \,/\, M; \qquad M = \frac{r_a}{r_s} \tag{5}$$

where M is the mass ratio and ρ_s is the solid density. The mass ratio is of the order of 10-3 as the density of vegetal material is typically 1000 times higher than the air density (de Langre, 2008). For the above mentioned Cauchy numbers, the reduced velocity in the current study may be ranging between 126 and 526. This explains why no resonance or lock-in was seen during the WoW tests as the reduced velocity is far from one (dynamical interaction such as resonance or lock-in is expected when UR is close to one). Furthermore, research carried out by Spatz et al. (2007) explains how trees escape dangerously large oscillations of the stem as the tree reacts to dynamic wind loads as a system of coupled damped oscillators. Damping in the elements (stem, primary branches and secondary branches) as well as soil-tree interaction is responsible for energy distribution within a tree. This results into a highly damped system which explains the tree's ability to escape dangerously large oscillations. The hypothesis of Spatz et al. (2007) is further supported by the research work carried out by Theckes et al. (2011) which explains damping-by-branches as a protective mechanism.

4.2 The question of scaling up the results for larger trees

The main focus of the current study was trees on buildings. The wind tunnel study had limited capability to scale up the loads to the larger size at the full-scale building. For this reason, the WoW tests were carried out, which allowed estimating the loads on trees with typical sizes at the full-scale building. The link between the wind tunnel and the WoW is missing basically due to shape change under wind speed. Such shape change and its associated effects on the wind load, was difficult to be compensated at the wind tunnel study. While wind loads on bluff bodies (solid objects) can be scaled up (Holmes, 2007), the methods may not be suitable for flexible objects such as trees because the response of small-scale models under constant wind speed conditions may not represent the response of large trees under actual wind conditions (Mayhead 1973, James, 2012). Rodriguez et al., (2008) hypothesized scaling laws based on the assumptions idealized allometric fractal trees and symmetric modes of branches. Scaling up the results of the WoW for larger trees requires further research in which different scaling parameters are needed. The larger trees might have different modulus of elasticity and hence different natural frequencies which might require monitoring of large trees under natural wind events. The response of trees to wind can vary according to the tree's size, age and specie. In addition, turbulence that was not available at the WoW may have some significant effects on the peak values of the wind loads. Future research may consider these limitations to further the understanding of the wind effects on large and full-scale trees at different ages and for different species.

5. Conclusions

An experimental study for the evaluation of wind loads on trees for vegetated building envelopes was carried out on small-scale models (boundary-layer wind tunnel tests) and full-scale actual species (open-jet testing). While the small-scale study permits understanding the interference effects from surrounding structures (global effects), the larger tree study allows the investigation of the wind-tree interaction and shape change (with wind speed change) effects (local effects) on the load coefficients. The results show that small-scale testing, which does not account fully for wind-tree interaction, may overestimate wind loading on trees. The full-scale testing results show that at higher wind speeds the total loading coefficients tend to be reduced, limiting the wind loads on trees. No resonance or vortex shedding was visually observed. The tree leaves/branches reduced the creation of a coherent vortex shedding and dampened all kinds of potential instability, and tree flexibility allowed significant deflections without failure. This may be attributed to the relatively high reduced velocity range (126-526), which covers a range of full-scale wind speed of 12.8-53 m/s, and porosity of the tree. Future research may consider scaling up the results of the full-scale for larger trees on the ground. It would be valuable repeating the same full-scale test in a turbulent flow.

References

Aly, A.M., Gan Chowdhury, A., and Bitsuamlak, G. (2011a), "Wind profile management and blockage assessment for a new 12-fan WoW facility at FIU", Wind Struct., **14**(4), 285-300.

Aly, A.M., Bitsuamlak, G. and Gan Chowdhury, A., (2011b), "Florida International University's Wall of Wind: a tool for the improvement of code provisions and design criteria for hurricane-prone regions", Vulnerability, Uncertainty, and Risk: Analysis, Modeling, and Management - Proceedings of the ICVRAM 2011 and ISUMA 2011 Conference, Hyattsville, MD, USA, April, pp. 352-359.

Aly, A.M., Bitsuamlak, G.T. and Gan Chowdhury, A. (2012), "Full-scale aerodynamic testing of a loose concrete roof paver system," Eng. Struct., **44**, 60-270.

Baycan-Levent, T. and Nijkamp, P. (2009), "Planning and management of urban green spaces in Europe: comparative analysis", J. Urban Plann. Dev., 135(1), 1–12.Blevins, R.D. (1990), *Flow-Induced Vibrations,* New York, Van Nostrand Reinhold.

de Langre, E. (2008), "Effects of wind on plants", Annu. Rev. Fluid Mech., (**40**), 141-168.

Diener, J., Rodriguez, M., Baboud, L. and Reveret, L. (2009), "Wind projection basis for real-time animation of trees", Comput. Graphics Forum*,* **28**(2), 533-540.

French, A. P. (1970), *Newtonian Mechanics*, The M.I.T. Introductory Physics Series, 1st ed., W. W. Norton and Company Inc., New York.

Gilman, E.F., Masters, F. and Grabosky, J. (2008), "Pruning affects tree movement in hurricane force wind", Arboric. Urban For., **34**(1):20–28.

Haritos, N. and James, K. (2008), "Dynamic response characteristics of trees from excitation by turbulent wind", 20th Australasian Conference on the Mechanics of Structures and Materials, ACMSM20, Toowoomba, Queensland, Australia, December.

Hough, M. (1984), *City form and natural processes*, Croom Helm, London.Hu, X., Tao, W. and Guo, Y. (2011), "Fluid-structure interaction simulation of a tree swaying in wind field", Chin. J. Comput. Mech.*,* **28**(2), 302-308.
Hu, X., Tao, W. and Guo, Y. (2008a), "Simulation of swaying tree in wind field considering coupling effect", J. Zhejiang Univ. (Eng. Sc.), **42**(7), 1123-1127.
Hu, X., Tao, W. and Guo, Y. (2008b), "Using FEM to predict tree motion in a wind field", J. Zhejiang Univ-Sc A, **9**(7), 907-915.
James, K.R. (2003), "Dynamic loading of trees", J. Arboric. **29**(3).
James, K.R., Haritos, N. and Ades, P. (2006), "Mechanical stability of trees under dynamic loads", Am. J. Bot. **93**(10), 1522-1530.
James, K.R. 2012, *A Dynamic Structural Analysis of Trees Subject to Wind Loading,* PhD thesis, University of Melbourne. Kontogianni, A., Tsitsoni, T. and Goudelis, G. (2011), "An index based on silvicultural knowledge for tree stability assessment and improved ecological function in urban ecosystems", Ecol. Eng., **37**(6), 914-919.
Mayhead, G.J. (1973), "Some drag coefficients for British trees derived from wind tunnel studies", Agric. Meteorology., 12,123-130.
Lin, D., Chen, C., Tang, L., Wang, Q. and Xu, W. (2009), "Interactive physical based animation of tree swaying in wind", 10th ACIS Conference on Software Engineering, Artificial Intelligence, Networking and Parallel/Distributed Computing, SNPD 2009, In conjunction with IWEA 2009 and WEACR 2009, Daegu, Korea, May.
Rodriguez, M., de Langre, E. and Moulia, B. (2008), "A scaling law for the effects of architecture and allometry on tree vibration modes suggests a biological tuning to modal compartmentalization", Am. J. Bot. **95**(12), 1523-1537.
Sellier, D. and Fourcaud, T. (2009), "Crown structure and wood properties: influence on tree sway and response to high winds", Am. J. Bot. **96**(5), 885-896.
Spatz, H.C, Bruchert, F. and Pfisterer, J. (2007), "Multiple resonance damping or how do trees escape dangerously large oscillations", Am. J. Bot. **94**(10), 1603-1611.
Theckes, B., de Langre, E. and Boutillon, X. (2011), "Damping by branching: a bioinspiration from trees", Bioinsp. Biomim. **(6)**, 1-11.
Zubizarreta-Gerendiain, A., Pellikka, P., Garcia-Gonzalo, J., Ikonen, V. and Peltola, H. (2012), "Factors affecting wind and snow damage of individual trees in a small management unit in Finland: assessment based on inventoried damage and mechanistic modeling", Silva Fenn., **46**(2), 181-196.

Tables

Table 1 Dimensions of actual trees used for the WoW testing.

identification	species name	height, m	width, m	projected area, m^2
tree # 1	Gumbo Limbo	4.267	1.829	1.951
tree # 2	Bay Rum	4.216	1.092	2.302
tree # 3	Green Buttonwood	3.353	1.372	—
tree # 4	Pigeon Plum	3.454	1.422	2.947

Table 2 List of test wind speeds, characteristics dimension, and the corresponding Reynolds numbers for small- and full-scale test sets.

test model size	U (m/s)	characteristic dimension (m)	Re
small-scale	6.3	0.036	1.43×10^4
large-scale	12.8	1.422	1.18×10^6
	26.2	1.422	2.42×10^6
	40.0	1.422	3.69×10^6
	43.1	1.422	3.97×10^6
	46.3	1.422	4.27×10^6
	49.5	1.422	4.56×10^6
	53.0	1.422	4.89×10^6

Table 3 Summary of Phase 2 vertical safety strand tension force (tree # 3 was used in this table).

Vel	Dir, (deg)	Dur. (sec)	4x4	mean (N)	rms (N)
12.8	0	180	Yes	46.7	2.7
26.2	0	180	Yes	162.8	11.1
40.0	0	180	Yes	408.4	27.1
43.1	0	10	Yes	456.8	16.5
46.3	0	10	Yes	510.7	20.0
49.5	0	10	Yes	577.0	21.8
53.0	0	10	Yes	645.9	19.1
12.8	0	180	No	59.2	4.4
26.2	0	180	No	239.3	9.3
40.0	0	180	No	491.5	16.9
43.1	0	10	No	507.1	13.8
46.3	0	10	No	574.3	15.6
49.5	0	10	No	638.8	15.1
53.0	0	10	No	705.5	16.5
12.8	90	180	Yes	13.3	1.8
26.2	90	180	Yes	73.8	4.0
40.0	90	180	Yes	277.1	12.9
12.8	90	180	No	22.2	2.7
26.2	90	180	No	85.4	4.9
40.0	90	180	No	192.2	9.8

Figures

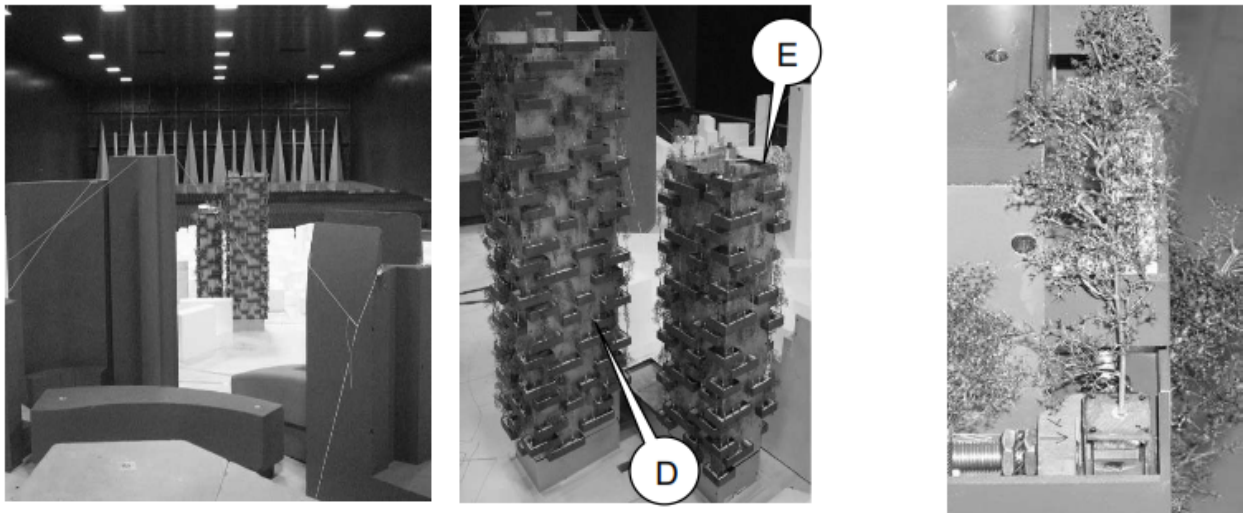

(a) Trees on tall buildings (towers D and E) **(b)** Tree on force balance

Fig. 1 Small-scale trees mounted on two tall buildings (towers D and E) tested in the boundary-layer wind tunnel of the Politecnico di Milano.

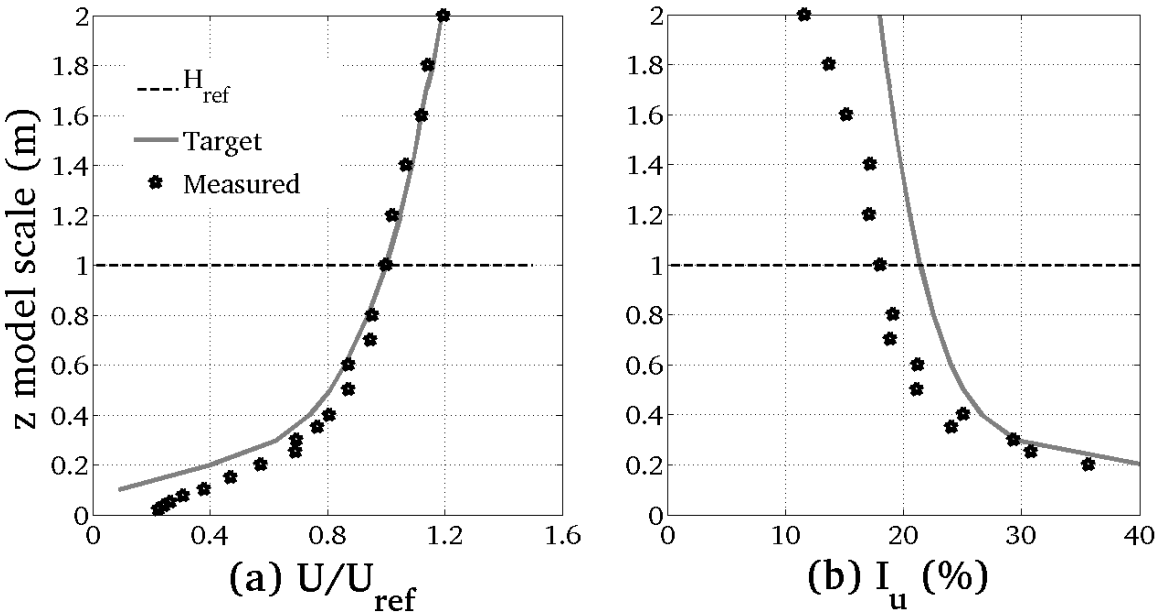

Fig. 2 Small-scale boundary-layer wind tunnel profile used in the current study: (a) mean wind speed profile, (b) turbulence intensity profiles.

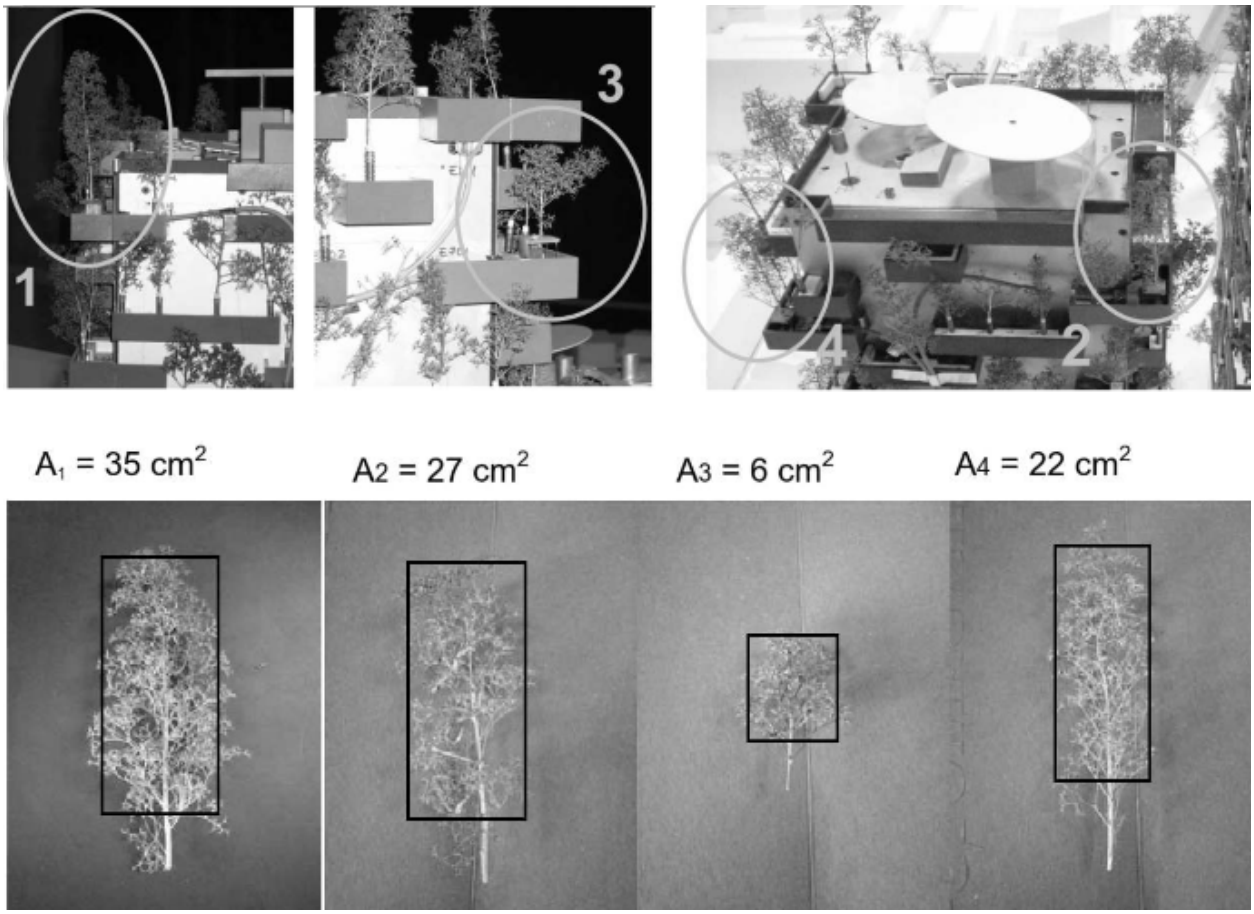

Fig. 3 Location and shape (projected areas) of four small-scale trees used for load coefficients calculations.

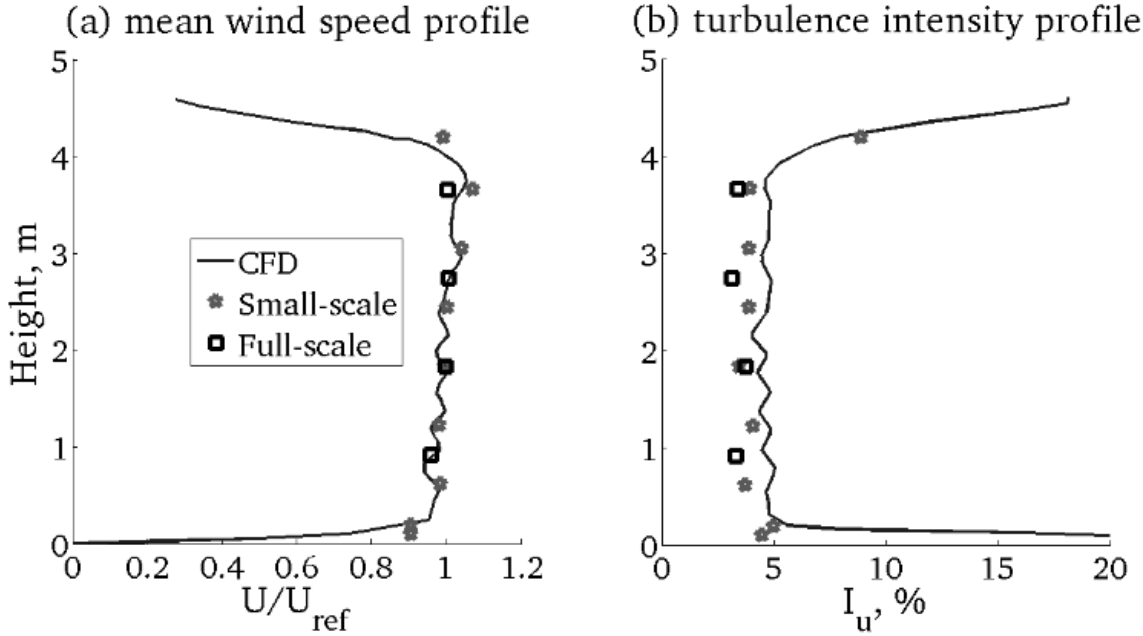

Fig. 4 Large-scale WoW profile used in the current study: (a) mean wind speed profile, (b) along-wind turbulence intensity profile.

(a) (b) (c) (d)

Fig. 5 Large-scale trees tested in the present study: (a) tree # 1: Gumbo Limbo (*Bursera simaruba*), (b) tree # 2: Bay Rum (*Pimenta recemosa*), (c) tree # 3: Green Buttonwood (*Conocarpus erectus*), and (d) tree # 4: Pigeon Plum (*Coccoloba diversifolia*)

(a) (b)

Fig. 6 Full-scale WoW testing (Phase 1): (a) steel frame mounted on load cells and (b) the overall test set in the test section.

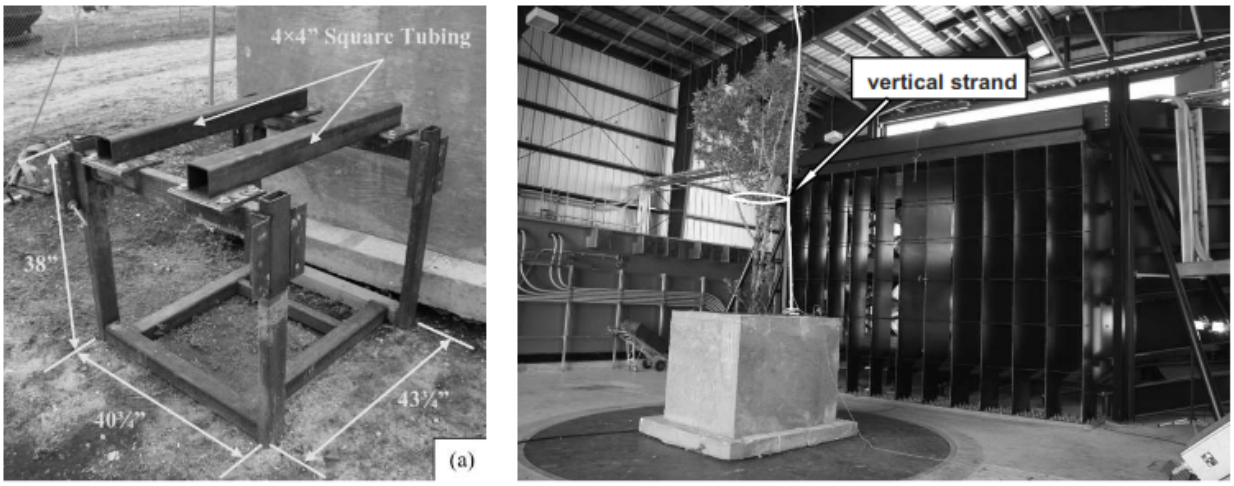

Fig. 7 Full-scale testing Phase 2: (a) steel cage proposed for securing the tree in the concrete box and (b) the full-scale tree in a reinforced concrete box as a representative sectional model of the full-scale balcony.

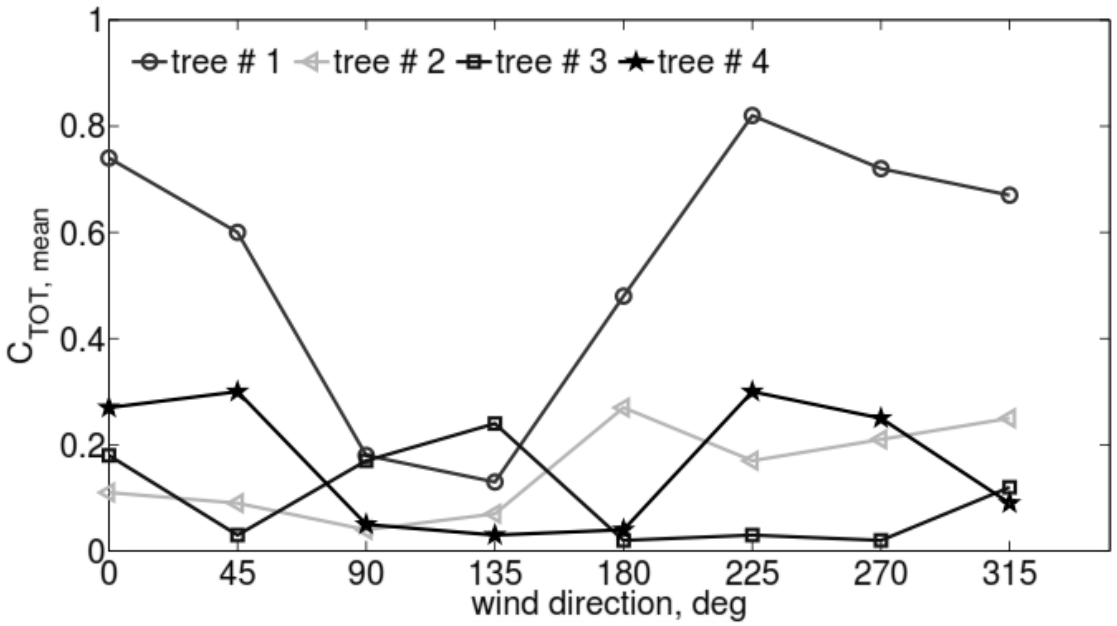

Fig. 8 Mean total force coefficient versus wind direction angle for small-scale trees tested in the boundary-layer wind tunnel test section (Re = 1.43 x 10^4).

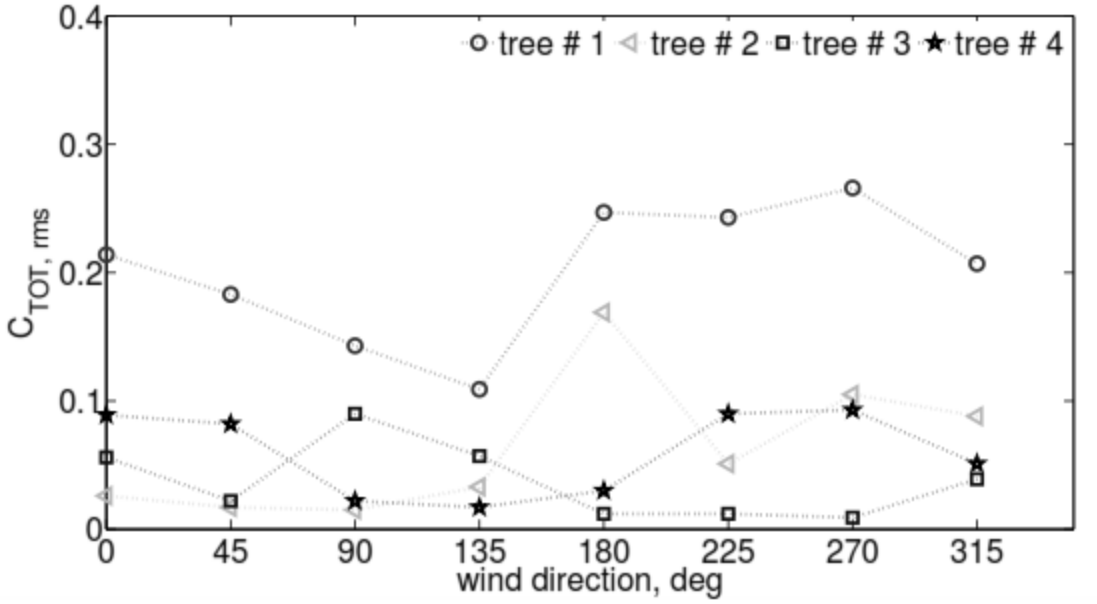

Fig. 9 Root mean square total force coefficient versus wind direction angle for small-scale trees tested in the boundary-layer wind tunnel test section (Re = 1.43 x 10^4).

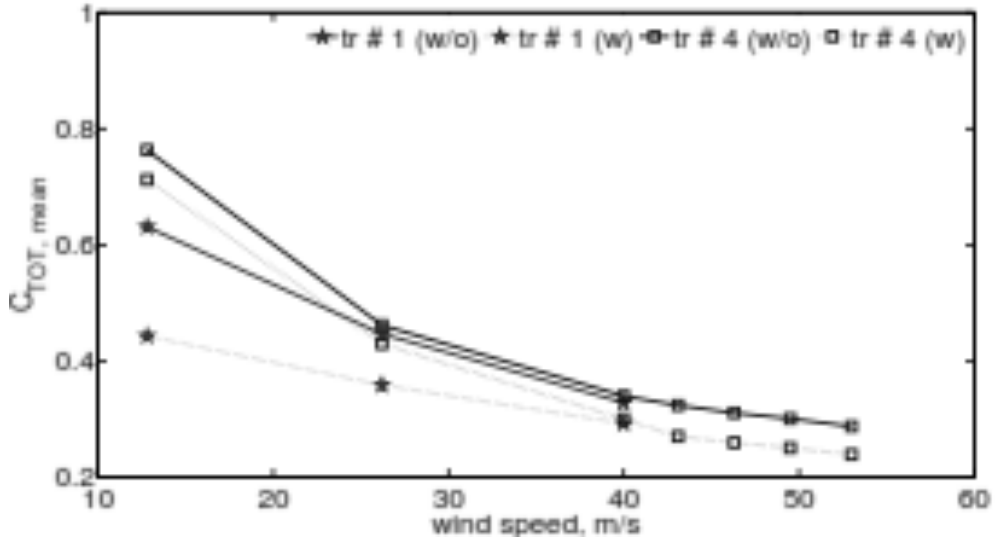

Fig. 10 Mean total force coefficient versus wind speed for large-scale trees tested at the WoW (Re varies from 1.18 x 10^6 to 4.89 x 10^6). In the legend, 'w/o' indicates that the safety cable was not attached to the tree while 'w' designates that the safety cable was connected to the tree which resulted in a reduction in the total force coefficient.

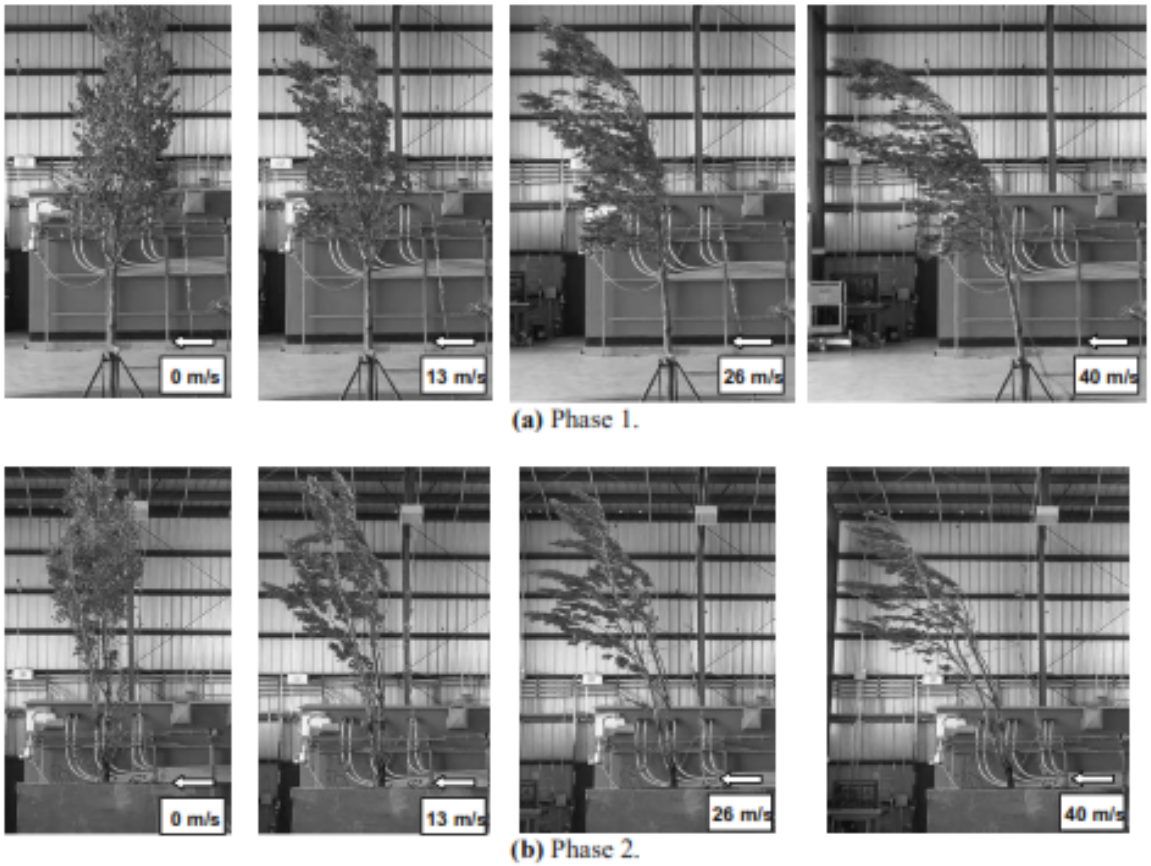

Fig. 11 Lateral photographs of actual trees at 0, 13, 26, and 40 m/s: (a) Phase 1; (b) Phase 2.

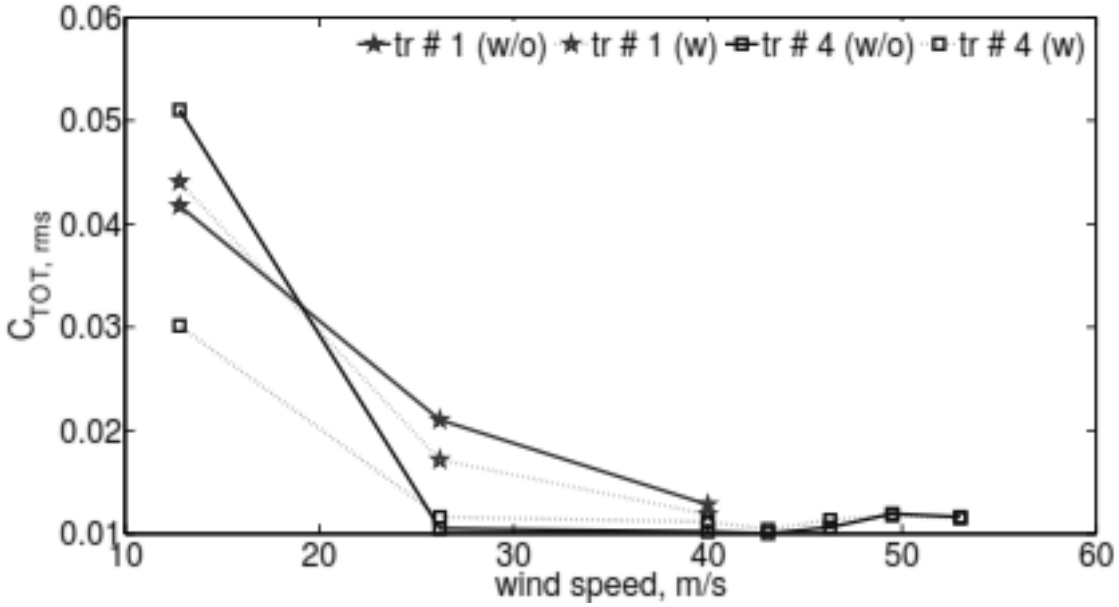

Fig. 12 Root mean square total force coefficient versus wind speed for large-scale trees tested at the WoW (Re varies from 1.18×10^6 to 4.89×10^6).

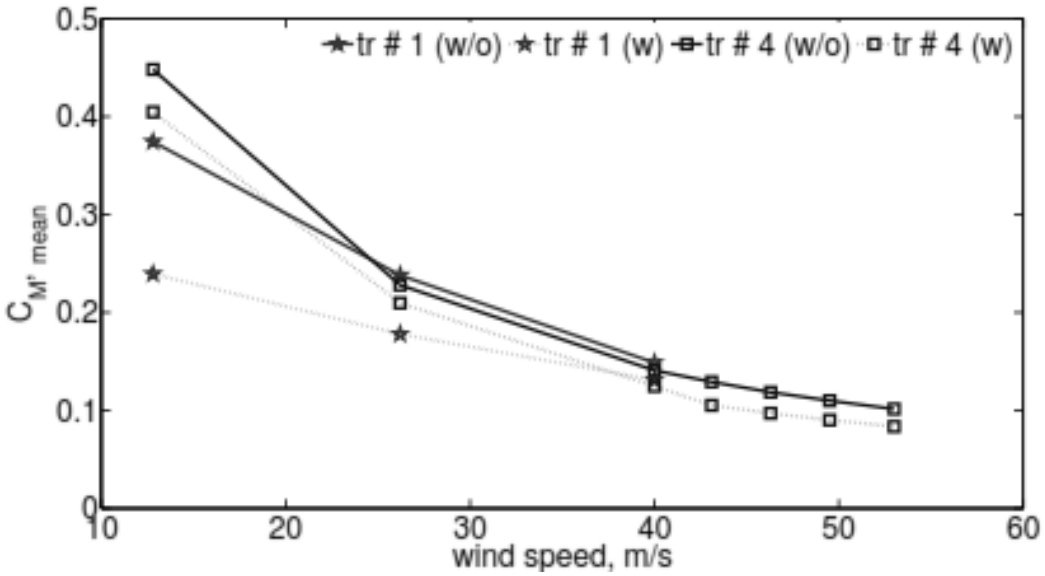

Fig. 13 Mean moment coefficient C_M versus wind speed for large-scale trees tested at the WoW (Re varies from 1.18 x 10^6 to 4.89 x 10^6). In the legend, 'w/o' means that the safety cable was not attached to the tree while 'w' designates that the safety cable was connected to the tree which resulted in a reduction in the total force coefficient.

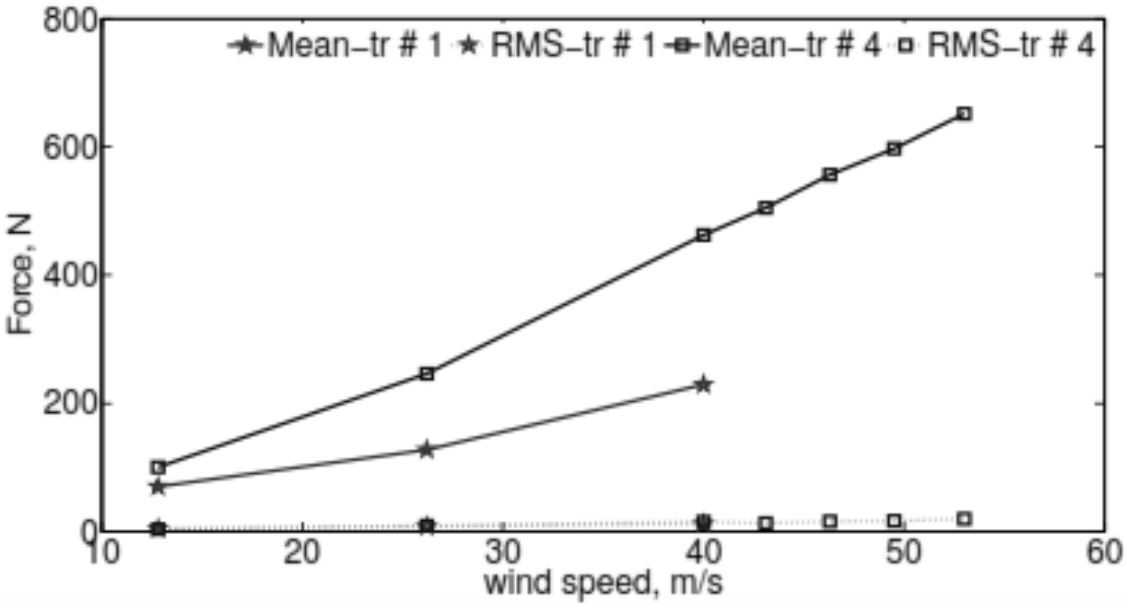

Fig. 14 Tension force created in the vertical safety cable versus wind speed for large-scale trees tested at the WoW.

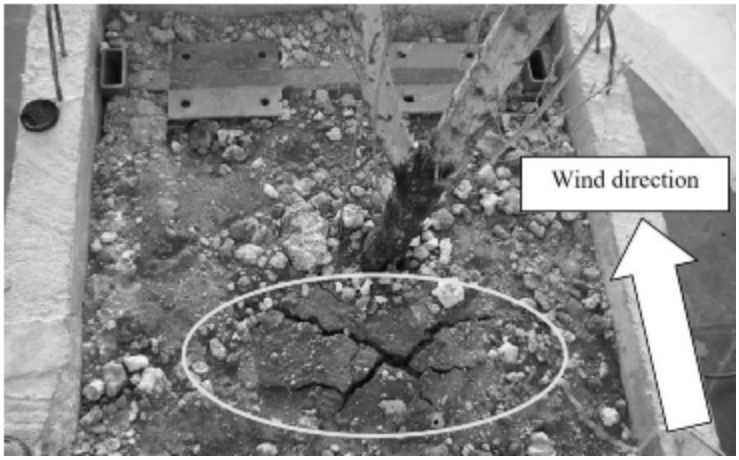

Fig. 15 Minor cracks were noticed during the high-speed tests of Phase 2. This represents the worst observed soil cracking during Phase 2 testing. It represents a test case with 90° wind direction without the vertical safety strand and the top 4×4” steel members installed on the steel frame inside the concrete planter box.